

Intermediate spectral statistics in the many-body localization transition

Piotr Sierant¹ and Jakub Zakrzewski^{1,2}

¹ *Institut Fizyki imienia Mariana Smoluchowskiego, Uniwersytet Jagielloński, ulica Profesora Stanisława Łojasiewicza 11, PL-30-348 Kraków, Poland*

² *Mark Kac Complex Systems Research Center, Uniwersytet Jagielloński, ulica Profesora Stanisława Łojasiewicza 11, PL-30-348 Kraków, Poland**

(Dated: May 16, 2022)

Spectral statistics of systems that undergo many-body localization transition are studied. An analysis of the gap ratio statistics from the perspective of inter- and intra-sample randomness allows us to pin point differences between transitions in random and quasi-random disorder, showing the effects due to Griffiths rare events for the former case. It is argued that the transition for a random disorder exhibits universal features that are identified by constructing an appropriate model of intermediate spectral statistics which is a generalization of the family of short-range plasma models. The model incorporates the inter- and intra-sample fluctuations and faithfully reproduces level spacing distributions as well as number variance during the transition from ergodic to many-body localized phase. In particular, it grasps the critical level statistics which arise at disorder strength for which the fluctuations are the strongest.

Many-body localization (MBL) seems to be the most robust manifestation of ergodicity breaking in the quantum world attracting enormous interest (for recent reviews see [1, 2] as well as a topical issue of *Annalen der Physik* [3]). From the early days of MBL systems were often characterized by level spacing distributions known from random matrix [4] and quantum chaos studies [5]. It has been realized [6] that the level unfolding (necessary to obtain a unit mean density of states) is a tricky procedure that, done naively, may affect the results. Instead a dimensionless ratio of consecutive energy levels gaps (referred as the gap ratio) was introduced [6]. It is defined as $r_n = \min\{\delta_n, \delta_{n-1}\} / \max\{\delta_n, \delta_{n-1}\}$ where $\delta_n = E_{n+1} - E_n$ is an energy difference between two consecutive levels.

The average gap ratio, \bar{r} , is different for fully extended systems (in the following we shall concentrate on the gaussian orthogonal ensemble (GOE) for time-reversal invariant systems) $\bar{r}_{GOE} \approx 0.53$ and for localized systems $\bar{r}_{Poi} \approx 0.39$ [6]. That property was used by many authors in attempts to localize the transition [7–13]. It has been possible to obtain analytic predictions for distributions of r both for GOE (in a simplified small matrix approach) and for the Poisson random sequence [14].

The latter limit seems highly relevant as it has been found that for MBL systems an extensive set of local integrals of motion exists making these systems integrable [1, 15, 16]. Therefore the delocalized, ergodic – MBL integrable transition resembles to some extent a similar transition between classically chaotic and classically integrable systems in quantum chaos studies [5]. Importantly, however, while the transition of a given low dimensional system from integrable limit to chaos when some external parameter (e.g. magnetic field in the hydrogen atom [17]) is varied is systems specific and closely determined by the structure of system specific periodic orbits [18], for MBL system the set of local integrals of mo-

tion (LIOM) depends on the disorder realization. Therefore, averaging over disorder implies averaging over different sets of LIOMs. Thus, contrary to system specific chaotic to integrable transitions, one may argue that ergodic to many-body localized transition may have universal statistical features. Especially, as it is to some extent successfully described by renormalization group picture [19, 20]. On the other hand, it has been postulated that the universality class of the transition depends on the disorder type [21, 22] identifying intra-sample randomness as the dominant feature for quasiperiodic disorder (QPD) while the inter-sample randomness being essential for purely random disorder (RD). Those important observations were made studying the entanglement entropy behavior.

The aim of this communication is twofold. Firstly, we show that a proper analysis of gap ratio statistics allows us to get similar insight on the randomness of system in MBL transitions as the entanglement entropy [21]. Our method is conceptually simpler as it relies only on the spectrum of the system and as such can be straightforwardly used in studies of various complex systems. Secondly, this analysis, as a by-product, gives hints on the construction of universal statistics for MBL transition which we provide generalizing earlier attempts [23–25]. *The gap ratio analysis.* The usual way of calculating the mean gap ratio \bar{r} is to average the r_n variable over a certain number of energy levels getting a mean gap ratio for one sample $r_S = \langle r_n \rangle_S$. Then, the mean gap ratio is obtained by averaging of r_S over disorder realizations $\bar{r} = \langle r_S \rangle_{dis}$. While, as mentioned above \bar{r} obtained in this way reflects the character of eigenstates of the system [6–12] a part of information encoded in the r_n variables is necessarily lost. Let us examine $P(r_S)$ – the distribution of the r_S – it provides a direct information about variations of the r_S for different disorder realizations. As an example we consider the XXZ spin chain with additional

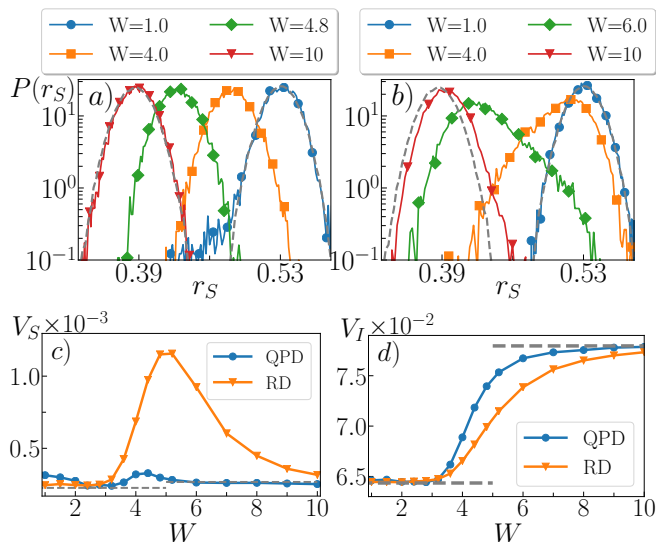


Figure 1: Top: (a) the distributions $P(r_S)$ for quasi-periodic disorder (QPD) of strength W . Dashed lines give limiting GOE and Poisson behaviors. The tail of the $W = 1$ distribution indicates that QPD reproduces GOE statistics only approximately; (b) the distributions $P(r_S)$ for random disorder (RD). Bottom: (c) the inter-sample variance V_S for RD and QPD; (d) the intra-sample variance V_I for QPD and RD during the transition.

next-nearest-neighbors coupling (similar to that of [21])

$$H = J \sum_i \vec{S}_i \cdot \vec{S}_{i+1} + W \sum_i \cos(2\pi\zeta i + \phi) S_i^z + J_1 \sum_i S_i^z S_{i+2}^z, \quad (1)$$

where $\vec{S}_i = \frac{1}{2}\vec{\sigma}$, $\zeta = (\sqrt{5} - 1)/2$ (the golden ratio) and ϕ is a fixed phase for a given disorder realization (leading to QPD) or is random on each lattice site (leading to RD with the same on-site distribution, as in the QPD case) [21]. We fix $J = 1$ as the energy unit and we study the case of $J_1 = J$ first. For the system size $L = 16$ we consider sequences of $N = 400$ consecutive eigenvalues from the middle of the spectrum yielding a collection of r_S values for $n_{dis} = 2000$ disorder realizations. The resulting distributions, $P(r_S)$, for different disorder strengths W are shown in Fig. 1.

Had all r_n been independent of each other the distribution of $r_S = \sum_{n=1}^N r_n/N$ should be Gaussian with width determined by the variance of the r_n distribution and proportional to $1/\sqrt{N}$. Despite the correlations – particularly strong for GOE – the $P(r_S)$ are Gaussian in the limiting cases of GOE and Poisson statistics. Surprisingly, the $P(r_S)$ distributions remain Gaussian for QPD across the transition.

In a striking contrast, the distributions in the RD case become strongly asymmetric with enlarged variance in the transition region. This reflects the inter-sample randomness importance for the RD and is a clear, nice manifestation of the existence of rare Griffiths regions [26–29]:

for samples with \bar{r} close to GOE there exist realizations of disorder leading to r_S close to Poisson limit. Similarly, on a localized side for \bar{r} close to integrable limit there are rare events with r_S values close to GOE value. The stark difference in the $P(r_S)$ distributions between the RD and QPD cases can be quantified by calculating a variance: $V_S = \langle r_S^2 - \bar{r}^2 \rangle_{dis}$. As Fig. 1(c) shows, the inter-sample variance V_S has a clear peak in the MBL transition for the RD whereas it varies only slightly for the QPD.

Consider now the variance v_I of the r_S variable, $v_I = \langle r_n^2 - r_S^2 \rangle_S$. Averaged over disorder realizations $V_I = \langle v_I \rangle_{dis}$, it provides information about fluctuations of r_n within a single spectrum of the system at a certain disorder strength – characterizing intra-sample randomness. As could be expected from the long range correlations of GOE, it is small for GOE and conversely, it is maximal for Poissonian spectrum. Fig. 1(d) shows that it behaves similarly for QPD and RD interpolating between the values for GOE and Poisson statistics. The transition is sharper for the system with QPD, implying that it is less affected by finite size effects [21].

Seeing that the distribution $P(r_S)$ and the variances V_S and V_I provide a valuable information about the randomness at the MBL transition, let us switch our attention to the more standard Heisenberg chain case taking $J_1 = 0$ in Eq. (1) and assuming random uniform disorder so that $\cos(2\pi\zeta i + \phi)$ is exchanged by $h_i \in [-1, 1]$ in Eq. (1). Despite the fact that the distribution of disorder is different and the studied model contains now nearest neighbor couplings only, the $P(r_S)$ behaves quite similarly to the case shown in Fig. 1(b) revealing strong asymmetry and broadening across the transition. Particularly, the broader distributions in the transition regime suggest that one may use the maximal variance V_S as an indicator of the transition point.

A standard finite size scaling of different quantities can be performed assuming $W \rightarrow (W - W_C)L^{1/\nu}$. For \bar{r} such an analysis has been performed already [9, 30] with the data collapsing to a single curve. Similar scaling may be used for the variance V_S . Observe that both the position of the maximum as well as its value depend on the system size – Fig. 2(a). If, together with the rescaling of the disorder strength, the variance V_S is rescaled according to $V_S \rightarrow \tilde{V}_S = (V_S - V_{GOE})/L^\kappa$ (where V_{GOE} is the inter-sample variance for GOE) the data for various system sizes collapse onto a single curve – Fig. 2(c) for the exponents $\nu = 0.95(10)$, $\kappa = 1.2(1)$ and the critical disorder strength $W_C = 3.5(1)$. The scaling of the V_S will necessarily cease to work for larger system sizes as the support of the $P(r_S)$ distribution is limited by \bar{r}_{Poi} and \bar{r}_{GOE} . On the other hand, the critical disorder strength $W_C = 3.5(1)$ and the exponent $\nu = 0.95(10)$ are in nice agreement with results of [9]. A similar finite size scaling may be performed for the intra-sample variance V_I with the same W_C and ν – Fig. 2(d). It is notable that all three measures \bar{r} , V_S and V_I scale in a very similar

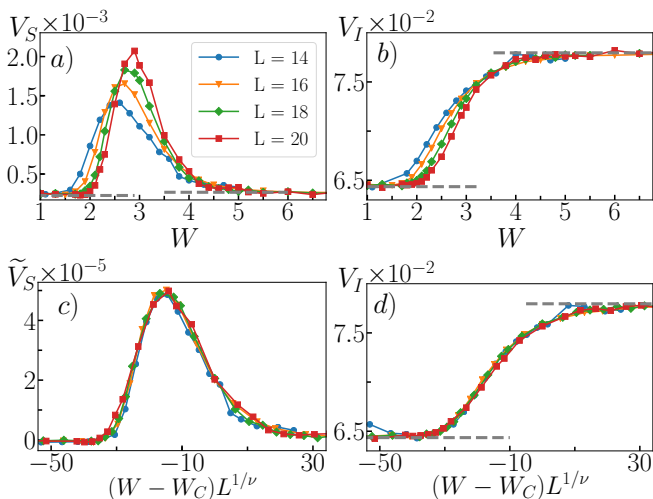


Figure 2: Top: (a) The variance V_S of the r_S distribution characterizing the inter-sample randomness; (b) the variance V_I reflecting the intra-sample fluctuations in the spectrum of the system. Bottom: (c) the rescaled inter-sample variance \tilde{V}_S and (d) the intra-sample variance V_I collapse after the rescaling of the disorder strength with $W_C = 3.5$ and $\nu = 0.95$. Data for system sizes $L \in \{14, 16, 18, 20\}$.

manner. Being interconnected they still provide different insights into physics of the system during the MBL transition.

Critical level statistics. We assume that the critical level statistics in MBL transition can be extracted from data for a system of size L for disorder strength W_L that maximizes the inter-sample variance V_S , e.g. $W_L = 2.7$ for $L = 16$. The finite size analysis assures that in the thermodynamic limit $L \rightarrow \infty$ $W_L \rightarrow W_C = 3.5(1)$. The critical statistics obtained in this way is presented in Fig. 3. It is almost system size independent within the available system sizes. To get the critical level spacing distribution $P(s)$ and the number variance $\Sigma^2(L)$ we had to unfold the spectra carefully (using the same procedure as in [31]). Only then one may compare the data with a theoretical model. Previous attempts used either a mean field plasma model [24] or different variants of critical statistics [25] known from single particle studies [32–34].

We consider a family of short-range plasma models (SRPMs) [35] describing eigenvalue distributions with logarithmic interactions only among a finite number h of neighboring eigenvalues. This model interpolates between GOE statistics for which $h \rightarrow \infty$ and the Poisson statistics for which the eigenvalues are uncorrelated (hence $h = 0$). The SRPM have exponential tails of the level spacings distributions $P(s) \propto \exp(-(h\beta + 1)s)$ and asymptotically linear number variance $\Sigma^2(L) \propto L/(h\beta + 1)$. However, the $P(r_S)$ distribution for critical level statistics has a broad and slightly asymmetric shape while the distribution for SRPM is a narrow Gaussian denoted with the violet line in Fig. 4a). Thus, the

pure SRPM cannot account for the inter-sample variance correctly. This also means that the exponential tail of the critical level spacing distribution is not reproduced accurately – similar holds for other quantities e.g. the number variance $\Sigma^2(L)$.

The basic feature of the transition observed above is the broad $P(r_S)$ distribution (reflecting Griffiths regions and probably to some extent also finite size effects). An attempt to model such a situation by a simple random matrix model seems fruitless. Instead, we construct an ensemble which is a mixture of different SRPMs – we dub our procedure a weighted SRPM (wSRPM). Let $\mathcal{P}_h^\beta(E_1, \dots, E_N)$ be a joint probability distribution function (JPDF) of all eigenvalues for SRPM characterized by h and β . A JPDF for wSRPM statistics is obtained as

$$\mathcal{P}_{wSRPM}(E_1, \dots, E_N) = \sum_i c_i \mathcal{P}_{h_i}^{\beta_i}(E_1, \dots, E_N) \quad (2)$$

where h_i and β_i range over an appropriate set of values and c_i are weight coefficients ($\sum_i c_i = 1$). The level spacing distribution for wSRPM is a linear combination of level spacing distributions for SRPMs which are its ingredients: $P_{wSRPM}(s) = \sum_i c_i P_{h_i}^{\beta_i}(s)$. Other quantities for wSRPM such as n -level correlation functions and the number variance $\Sigma^2(L)$ are also linear combinations of appropriate quantities for SRPM which enter the JPDF of wSRPM.

The wSRPM model, defined above, is dependent on a large number of parameters $\{(h_i, \beta_i, c_i)\}$ that can be determined by requiring that $P_{wSRPM}(r_S) = \sum_{i=1}^{i_{max}} c_i P_{h_i}^{\beta_i}(r_S)$ reproduces the $P(r_S)$ distribution of the original model at given disorder strength W . Each of the SRPMs has its $P_h^\beta(r_S)$ distribution which is approximately Gaussian centered around a mean gap ratio \bar{r}_h^β which depends on h and β , we consider the set $\{(h_i, \beta_i)\}$ corresponding to $\bar{r}_{h_i}^{\beta_i}$ covering the interval $[\bar{r}_{Poi}, \bar{r}_{GOE}]$ approximately uniformly, that is we choose

$$(\beta_i, h_i) = \begin{cases} (\frac{i}{100}, 1), & i \in [0, 10], \\ (\frac{i-8}{20}, 1), & i \in [11, 30], \\ (1, i-30), & i \in [31, 30 + h_{max}]. \end{cases} \quad (3)$$

The weight coefficients c_i are obtained by minimizing the integral of the square of difference between $P_{wSRPM}(r_S)$ and $P(r_S)$ increased by a term $\sum_i (c_i - c_{i+1})^2/m$ which assures that the changes in the c_i coefficients are not too abrupt with i (the constant m is taken as 10^{-4} , changing the value by a factor of 5 only mildly affects the results). Fitting procedure defined in this way can be used to obtain wSRPMs for various system sizes and disorder strengths in the MBL crossover. Moreover, given the choice (3), the wSRPMs are determined by the minimum of a certain function of the weight coefficients c_i so there are actually no free parameters in the fitting procedure (besides the globally fixed m).

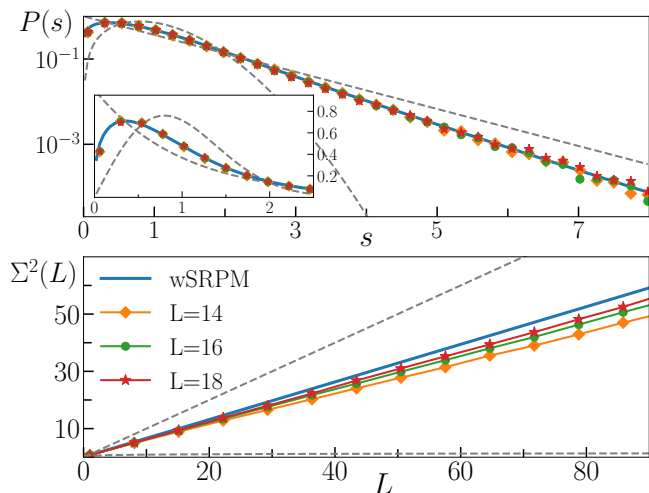


Figure 3: Critical level statistics for XXZ spin chain with random uniform disorder. Dashed lines correspond to the GOE and Poisson cases.

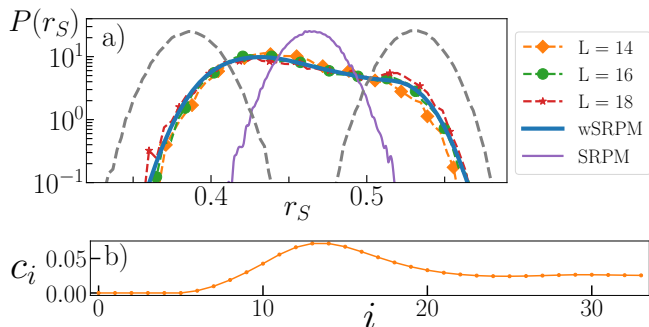


Figure 4: a) The $P(r_S)$ distribution for the critical statistics in XXZ spin chain along with wSRPM and $P(r_S)$ for SRPM. b) The c_i coefficients of wSRPM shown in Fig 3.

For a system close to the ergodic regime, we find that level statistics is a mixture of a dominant SRPM with $\beta = 1$ and varying $h > 1$ (which diverges as one approaches the ergodic regime) with small contribution of SRPMs with smaller h and β that account for disorder realizations for which the system has more localized properties. Upon approaching the MBL transition, the interactions between eigenvalues get more local and the weight of contributions with $h = 1$ and smaller values of β increases. Finally, as one gets closer to the MBL regime, the appropriate leading distribution is based on SRPMs with $\beta < 1$ with certain admixtures of SRPMs with stronger level repulsion β . Those contributions get gradually smaller and in the MBL phase there are no correlations between eigenvalues only SRPM with $\beta = 0$ contributes.

As the system size increases the statistics on the ergodic (MBL) side of crossover tend towards GOE (Poisson) limit, the width of the crossover diminishes. The

L	W	\bar{r}	χ
14	2.62	0.4528(4)	0.545(9)
16	2.7	0.4537(5)	0.587(5)
18	2.8	0.4569(7)	0.605(4)
		\bar{r}_{wSRPM}	χ_{wSRPM}
		0.4530	0.639

Table I: The average gap ratio \bar{r} and spectral compressibility χ for the XXZ spin chain at disorder strength which corresponds to W_C at $L \rightarrow \infty$. For comparison, the predictions of wSRPM r_{wSRPM} and χ_{wSRPM} are displayed.

critical level statistics which we conjecture to be relevant exactly in the MBL transition in large system size limit is presented in Fig. 3. The obtained wSRPM contains SRPMs with long-range interactions $h > 1$ (non-zero weights c_i with $i > 30$) together with dominating contribution of models with local interactions and $\beta < 1$. Large number of contributing SRPMs allows to accurately reproduce the $P(r_S)$ distribution (Fig. 4). Moreover, it is absolutely vital to faithfully reproduce the number variance. The values of spectral compressibility χ defined by the linear large L behavior of the number variance $\Sigma^2(L) \propto \chi L$ together with the average gap ratios \bar{r} are shown in Tab. I. This quantities are in good agreement with the predictions of the wSRPM \bar{r}_{wSRPM} and χ_{wSRPM} . The data suggest that the remaining small deviation in the spectral compressibility χ is probably a finite size effect.

A few remarks are in order. First, observe that the information about the admixture of systems with stronger localization properties is contained in the tail of $P(s)$ showing its significance. Let us also note that the relation between the exponential tail of $P(s)$ and the slope of number variance existing for the standard SRPM no longer holds if one considers the wSRPM – this allows the latter to fit the XXZ data with such a precision. Level spacing distribution $P_A(s)$ in the Anderson transition [23] combines level repulsion at small s characteristic for GOE and an exponential tail of Poisson level statistics, the critical statistics shown in Fig. 3 also possess the two features. However, the large inter-sample randomness encoded in broad $P(r_S)$ distribution is a crucial property of the critical level statistics in MBL transition, whereas it does not play a role in the Anderson transition (the $P_A(r_S)$ distribution has a Gaussian shape with width same as in the GOE and Poisson limits).

Conclusions and beyond. The gap ratio analysis demonstrates that more than just an overall information about the crossover between ergodic and MBL regimes can be obtained from the r_n variables. The considered inter- and intra-sample variances V_S and V_I reflect nicely the differences between RD and QPD universality classes. Furthermore, the $P(r_S)$ distribution quantifies the inter-sample fluctuations of a system undergoing MBL transi-

tion and gives a particularly clear demonstration of the Griffiths regime. On the other hand, it hints how to formulate the wSRPM model of spectral statistics across the MBL transition for the random disorder. The relevant ensemble is a mixture of short-range plasma models [35] allowing us to reproduce both the short-range (spacings, gap ratios) and the long range (number variance) spectral correlations. It is also interesting to find that the MBL transition for the QPD case cannot be described within this model. It supports the claim of [21] that the transitions for RD and QPD are of different universality classes. The ensemble that reproduces QPD MBL transition is yet to be identified.

This work was performed with the support of EU via Horizon2020 FET project QUIC (nr. 641122). Numerical results were obtained with the help of PL-Grid Infrastructure. We acknowledge support of the National Science Centre (PL) via project No.2015/19/B/ST2/01028 (P.S.), No.2018/28/T/ST2/00401 (Etiuda scholarship – P.S.) and the QuantERA programme No. 2017/25/Z/ST2/03029 (J.Z.).

* Electronic address: jakub.zakrzewski@uj.edu.pl

- [1] D. A. Huse, R. Nandkishore, and V. Oganesyan, *Phys. Rev. B* **90**, 174202 (2014), URL <http://link.aps.org/doi/10.1103/PhysRevB.90.174202>.
- [2] R. Nandkishore and D. A. Huse, *Ann. Rev. Cond. Mat. Phys.* **6**, 15 (2015).
- [3] *Annalen der Physik* **529** (2017), ISSN 1521-3889, URL <http://dx.doi.org/10.1002/andp.201770051>.
- [4] M. L. Mehta, *Random Matrices (Revised and Enlarged Second Edition)* (Elsevier, 1990).
- [5] F. Haake, *Quantum Signatures of Chaos* (Springer, Berlin, 2010).
- [6] V. Oganesyan and D. A. Huse, *Phys. Rev. B* **75**, 155111 (2007), URL <http://link.aps.org/doi/10.1103/PhysRevB.75.155111>.
- [7] A. Pal and D. A. Huse, *Phys. Rev. B* **82**, 174411 (2010), URL <http://link.aps.org/doi/10.1103/PhysRevB.82.174411>.
- [8] R. Mondaini and M. Rigol, *Phys. Rev. A* **92**, 041601 (2015), URL <http://link.aps.org/doi/10.1103/PhysRevA.92.041601>.
- [9] D. J. Luitz, N. Laflorencie, and F. Alet, *Phys. Rev. B* **91**, 081103 (2015), URL <https://link.aps.org/doi/10.1103/PhysRevB.91.081103>.
- [10] D. J. Luitz, N. Laflorencie, and F. Alet, *Phys. Rev. B* **93**, 060201 (2016), URL <http://link.aps.org/doi/10.1103/PhysRevB.93.060201>.
- [11] P. Sierant, D. Delande, and J. Zakrzewski, *Phys. Rev. A* **95**, 021601 (2017), URL <https://link.aps.org/doi/10.1103/PhysRevA.95.021601>.
- [12] P. Sierant and J. Zakrzewski, *New Journal of Physics* **20**, 043032 (2018), URL <http://stacks.iop.org/1367-2630/20/i=4/a=043032>.
- [13] J. Janarek, D. Delande, and J. Zakrzewski, *Phys. Rev. B* **97**, 155133 (2018), URL <https://link.aps.org/doi/10.1103/PhysRevB.97.155133>.
- [14] Y. Y. Atas, E. Bogomolny, O. Giraud, and G. Roux, *Phys. Rev. Lett.* **110**, 084101 (2013), URL <http://link.aps.org/doi/10.1103/PhysRevLett.110.084101>.
- [15] M. Serbyn, Z. Papić, and D. A. Abanin, *Phys. Rev. Lett.* **111**, 127201 (2013), URL <http://link.aps.org/doi/10.1103/PhysRevLett.111.127201>.
- [16] J. Z. Imbrie, *Phys. Rev. Lett.* **117**, 027201 (2016), URL <https://link.aps.org/doi/10.1103/PhysRevLett.117.027201>.
- [17] H. Friedrich and H. Wintgen, *Physics Reports* **183**, 37 (1989), ISSN 0370-1573, URL <http://www.sciencedirect.com/science/article/pii/037015738990121X>.
- [18] M. C. Gutzwiller, *J. Math. Phys.* **12**, 343 (1971).
- [19] A. C. Potter, R. Vasseur, and S. A. Parameswaran, *Phys. Rev. X* **5**, 031033 (2015), URL <https://link.aps.org/doi/10.1103/PhysRevX.5.031033>.
- [20] R. Vosk, D. A. Huse, and E. Altman, *Phys. Rev. X* **5**, 031032 (2015), URL <https://link.aps.org/doi/10.1103/PhysRevX.5.031032>.
- [21] V. Khemani, D. N. Sheng, and D. A. Huse, *Phys. Rev. Lett.* **119**, 075702 (2017), URL <https://link.aps.org/doi/10.1103/PhysRevLett.119.075702>.
- [22] S.-X. Zhang and H. Yao, *Phys. Rev. Lett.* **121**, 206601 (2018), URL <https://link.aps.org/doi/10.1103/PhysRevLett.121.206601>.
- [23] B. I. Shklovskii, B. Shapiro, B. R. Sears, P. Lambrianides, and H. B. Shore, *Phys. Rev. B* **47**, 11487 (1993), URL <https://link.aps.org/doi/10.1103/PhysRevB.47.11487>.
- [24] M. Serbyn and J. E. Moore, *Phys. Rev. B* **93**, 041424 (2016), URL <http://link.aps.org/doi/10.1103/PhysRevB.93.041424>.
- [25] C. L. Bertrand and A. M. García-García, *Phys. Rev. B* **94**, 144201 (2016), URL <https://link.aps.org/doi/10.1103/PhysRevB.94.144201>.
- [26] R. B. Griffiths, *Phys. Rev. Lett.* **23**, 17 (1969), URL <https://link.aps.org/doi/10.1103/PhysRevLett.23.17>.
- [27] T. Vojta, *Journal of Low Temperature Physics* **161**, 299 (2010), ISSN 1573-7357, URL <https://doi.org/10.1007/s10909-010-0205-4>.
- [28] K. Agarwal, S. Gopalakrishnan, M. Knap, M. Müller, and E. Demler, *Phys. Rev. Lett.* **114**, 160401 (2015), URL <https://link.aps.org/doi/10.1103/PhysRevLett.114.160401>.
- [29] K. Agarwal, E. Altman, E. Demler, S. Gopalakrishnan, D. A. Huse, and M. Knap, *Annalen der Physik* **529**, 1600326 (2017).
- [30] K. Kudo and T. Deguchi, *Phys. Rev. B* **97**, 220201 (2018), URL <https://link.aps.org/doi/10.1103/PhysRevB.97.220201>.
- [31] P. Sierant and J. Zakrzewski, *Weighted models for level statistics across the many-body localization transition* (2018), arXiv: 1808.02795, 1808.02795, URL <http://arxiv.org/abs/1808.02795>.
- [32] V. E. Kravtsov and K. A. Muttalib, *Phys. Rev. Lett.* **79**, 1913 (1997), URL <https://link.aps.org/doi/10.1103/PhysRevLett.79.1913>.
- [33] S. M. Nishigaki, *Phys. Rev. E* **59**, 2853 (1999), URL <https://link.aps.org/doi/10.1103/PhysRevE.59.2853>.
- [34] A. M. García-García and J. J. M. Verbaarschot, *Phys.*

Rev. E **67**, 046104 (2003), URL <https://link.aps.org/doi/10.1103/PhysRevE.67.046104>.

[35] Bogomolny, E., Gerland, U., and Schmit, C., Eur. Phys.

J. B **19**, 121 (2001), URL <https://doi.org/10.1007/s100510170357>.